International Journal of Smart Home
Vol.10, No.12 (2016), pp.25-34
http://dx.doi.org/10.14257/ijsh.2016.10.12.03

The Identification of Tool Eccentricity Parameters in Micro-Milling

Zhang Xiang and Wang Guanglin

School of Mechatronics Engineering, Harbin Institute of Technology, Heilongjiang Province, China
zhangxiang1982@hit.edu.cn

Abstract

Milling tool eccentricity has great influence in micro-milling. It could cause single edge cutting phenomenon, and effect machining quality and tool life. To recognize tool eccentricity parameters, on the basis of the tool eccentricity model, cutting edge trajectories are analyzed, and then a tool eccentricity identification method is proposed. The parameters of identification model are obtained by experiments and tool eccentricity parameters are calculated by iterative method. Finally, the accuracy of the proposed method is verified by measuring the diameter of a milled hole, and the verified result shows the proposed identification model is effective.

***Keywords**: Tool eccentricity, Single edge cutting phenomenon, Micro-milling*

1. Introduction

The diameters of the tool are between 0.1mm to 1mm in micro-milling [1], and tool eccentricity length is about 1μm to 10μm. Tool eccentricity has little effect in conventional milling. However, since the tool eccentricity and feed per tooth are in the same order of magnitude, tool eccentricity has great effect in micro-milling. Due to the impact of the tool eccentricity, instantaneous uncut chip thicknesses of different cutting edge are not equal in the same axial depth, or even only one cutting edge can remove material effectively, which is so-called single edge cutting phenomenon [2]. The instantaneous uncut chip thickness of the same edge changes with axial depth, because of tool eccentricity angle changes along with helix edge. Even in different axial depth, single edge cutting and two edges cutting alternates.

At the same time, the impact of tool eccentricity on surface roughness and tool life also cannot be overlooked [3]. Feng et al [4] and Tai et al [5] measured the tool eccentricity length and angle, respectively. Nakkiew et al [6] proposed a practical method in high speed end-milling which used an indicator of the tool eccentricity and need not reference sphere. The indicator is based on the size of milled marks, and then tool eccentricity parameters are obtained by quantitative precision analysis of those marks. Hekman et al [7] estimated magnitude and angle of tool eccentricity by time-dependent spectral analysis of the cutting force. In their model, tool eccentricity generates a cutting force component at spindle rotational frequency. Tool eccentricity characteristics are updated from cutting force, recursively. Wan et al [8] proposed three different tool eccentricity models to calculate the instantaneous uncut chip thickness, and then calibrate the cutting force model parameters and tool eccentricity parameters of peripheral milling. Their calibration model only needs one or two cutting test. The results show that their models are efficient and reliable. Ko et al [9] followed the movement of the tool center which varied with nominal feed, tool deflection and eccentricity, and calculate the relationship between instantaneous uncut chip thickness and cutting force coefficients. They contrast the predicted and measured cutting forces over a wide range of cutting conditions, and then recognize tool eccentricity. Zhang et al [10] established a micro-ball-end cutting force

ISSN: 1975-4094 IJSH

model, which takes into account the impact of tool eccentricity and the scale effects in micro-milling. Then iterative algorithm is used to calculate the minimum standard deviation square sums of cutting force coefficients, which tool eccentricity parameters could be considered as the actual parameters.

Therefore, this paper analyzed the tool path, which in view of tool eccentricity, and then proposed a tool eccentricity identification method which based on analytic geometry.

2. Tool Eccentricity Model

2.1 Definition of Tool Eccentricity

In this paper, tool eccentricity is total eccentricity which is due to manufacturing error and clamping error. In conventional milling, since the larger feed per tooth, tool eccentricity has less impact on milling process. However, since the cutting tool diameter is quite small in micro-milling, spindle speed should be larger than 30000 rpm in order to ensure sufficient cutting speed. Such spindle total eccentricity which is due to manufacturing error, clamping error and other factors is between 1 to 10 micrometers, as the same magnitude as feed per tooth in micro-milling, and will have a major impact to the trajectories of cutting edge and cannot be ignored. Tool eccentricity is indicated in Figure1. Definition of the distance between tool center and tool rotation center is tool eccentricity length (signed r in Figure 1); definition of the angle between tool eccentricity direction and Y-axis direction (when tool edges are parallel to Y-axis) is tool eccentricity angle (signed θ in Figure 1).

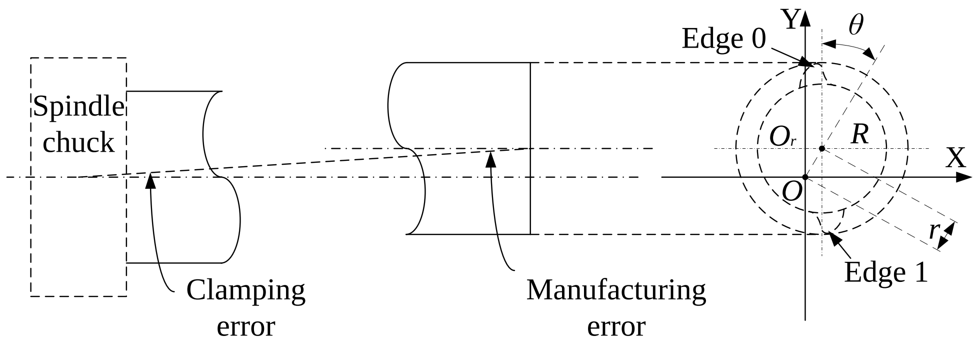

Figure 1. Schematic Diagram of Tool Eccentricity

2.2 Cutting Edge Trajectory Model

According to feed motion, rotary motion and tool eccentricity, the cutting edge trajectories equation is derived. In considering the motion characteristics of milling process, five Cartesian coordinate systems are established as shown in Figure 2.

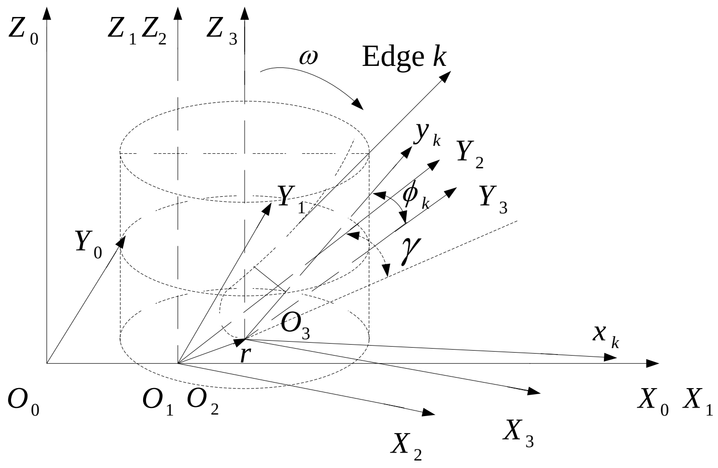

Figure 2. Edges Motion Trajectory Coordinate System

(1) Cartesian coordinate system $O_0X_0Y_0Z_0$, inertial reference system of the workpiece (workpiece coordinate system), fixed on the workpiece.

(2) Cartesian coordinates system $O_1X_1Y_1Z_1$, spindle translational coordinate system, moving with the spindle (feed movement), and the feed rate f in X_1-axis component, Y_1-axis and Z_1-axis are f_x, f_y, f_z, respectively.

(3) Cartesian coordinates system $O_2X_2Y_2Z_2$, spindle rotating coordinate system, rotating with Z_1-axis, and angular velocity is the actual angular velocity of the spindle.

(4) Cartesian coordinates system $O_3X_3Y_3Z_3$, tool local coordinate system, and its positive direction of X_3-axis keeps consistent with X_2-axis.

(5) Cartesian coordinates $O_3x_ky_kZ_3$, edge k local coordinate system, y_k-axis through edge k, and the angle between y_k-axis and Y_3-axis is Φ_k. From differential geometry, homogeneous coordinate expression of edge k is shown as follows:

$$\begin{bmatrix} x_k & y_k & z_k & 1 \end{bmatrix}^{\mathrm{T}} = \begin{bmatrix} 0 & R & z & 1 \end{bmatrix}^{\mathrm{T}} \tag{1}$$

In coordinates system $O_3X_3Y_3Z_3$, the expression of edge k could be obtained by rotation convert from coordinates system $O_3x_ky_kZ_3$, as shown in the following formula:

$$\begin{bmatrix} X_3 & Y_3 & Z_3 & 1 \end{bmatrix}^{\mathrm{T}} = M_{k3}(\phi_k)\begin{bmatrix} x_k & y_k & z_k & 1 \end{bmatrix}^{\mathrm{T}} \tag{2}$$

where, k is cutting edge number (k = 0, 1),

$$M_{k3}(\phi_k) = \begin{bmatrix} \cos\phi_k & -\sin\phi_k & 0 & 0 \\ \sin\phi_k & \cos\phi_k & 0 & 0 \\ 0 & 0 & 1 & 0 \\ 0 & 0 & 0 & 1 \end{bmatrix} \tag{3}$$

$$\phi_k = 2\pi k / K \tag{4}$$

where, K is the number of cutting edges (K=2, in this paper).

In coordinates system $O_2X_2Y_2Z_2$, the expression of edge k could be obtained by translational convert from coordinates system $O_3X_3Y_3Z_3$, by the following formula:

$$\begin{bmatrix} X_2 & Y_2 & Z_2 & 1 \end{bmatrix}^{\mathrm{T}} = M_{32}(r,\theta)\begin{bmatrix} X_3 & Y_3 & Z_3 & 1 \end{bmatrix}^{\mathrm{T}} \tag{5}$$

where,

$$M_{32}(r,\theta) = \begin{bmatrix} 1 & 0 & 0 & r\sin\theta \\ 0 & 1 & 0 & r\cos\theta \\ 0 & 0 & 1 & 0 \\ 0 & 0 & 0 & 1 \end{bmatrix} \tag{6}$$

Tool rotates around Z_1-axis in milling, and angular velocity is ω. In time t, the angle between Y_2-axis and Y_1-axis is ωt. The expression of edge k could be obtained by rotation convert from coordinates system $O_2X_2Y_2Z_2$, by the following formula:

$$\begin{bmatrix} X_1 & Y_1 & Z_1 & 1 \end{bmatrix}^{\mathrm{T}} = M_{21}(\omega,t)\begin{bmatrix} X_2 & Y_2 & Z_2 & 1 \end{bmatrix}^{\mathrm{T}} \tag{7}$$

where,

$$M_{21}(\omega,t) = \begin{bmatrix} \cos\omega t & \sin\omega t & 0 & 0 \\ -\sin\omega t & \cos\omega t & 0 & 0 \\ 0 & 0 & 1 & 0 \\ 0 & 0 & 0 & 1 \end{bmatrix} \tag{8}$$

Because of tool feed motion, translation distance components in X_0-axis, Y_0-axis and Z_0-axis are $f_x t$, $f_y t$ and $f_z t$ in time t, respectively. So, the expression of edge k could be obtained by translational convert of coordinates system $O_1X_1Y_1Z_1$, as shown in the following formula:

$$\begin{bmatrix} X_0 & Y_0 & Z_0 & 1 \end{bmatrix}^{\mathrm{T}} = M_{10}(f_x, f_y, f_z, t)\begin{bmatrix} X_1 & Y_1 & Z_1 & 1 \end{bmatrix}^{\mathrm{T}} \tag{9}$$

where,

$$M_{10}(f_x, f_y, f_z, t) = \begin{bmatrix} 1 & 0 & 0 & f_x t \\ 0 & 1 & 0 & f_y t \\ 0 & 0 & 1 & f_z t \\ 0 & 0 & 0 & 1 \end{bmatrix} \tag{10}$$

In summary, the total transformation matrix of edge k is:

$$M = M_{10}(f_x, f_y, f_z, t)M_{21}(\omega,t)M_{32}(r,\gamma_0)M_{k3}(\phi_k) \tag{11}$$

Thereby,

$$M = \begin{bmatrix} \cos(\omega t-\varphi_k) & \sin(\omega t-\varphi_k) & 0 & f_x t + r\sin(\omega t+\theta) \\ -\sin(\omega t-\varphi_k) & \cos(\omega t-\varphi_k) & 0 & f_y t + r\cos(\omega t+\theta) \\ 0 & 0 & 1 & f_z t \\ 0 & 0 & 0 & 1 \end{bmatrix} \tag{12}$$

The expression of edge k in workpiece inertial reference system is shown as:

$$\begin{bmatrix} X_0 & Y_0 & Z_0 & 1 \end{bmatrix}^{\mathrm{T}} = M\begin{bmatrix} x_k & y_k & z_k & 1 \end{bmatrix}^{\mathrm{T}} \tag{13}$$

And cutting edge trajectories equation is shown in following:

$$\begin{bmatrix} X_0 \\ Y_0 \\ Z_0 \\ 1 \end{bmatrix} = \begin{bmatrix} f_x t + R\sin(\omega t - 2\pi k/K) + r\sin(\omega t + \theta) \\ f_y t + R\cos(\omega t - 2\pi k/K) + r\cos(\omega t + \theta) \\ f_z t + z \\ 1 \end{bmatrix} \tag{14}$$

2.3 Effect of Tool Eccentricity

To simplify the model, it is assumed that feed direction coincides with the X-axis, and axial component of feed velocity f_z is ignored. According to equation (14), cutting edge trajectories could be drawn as shown in Figure 3.

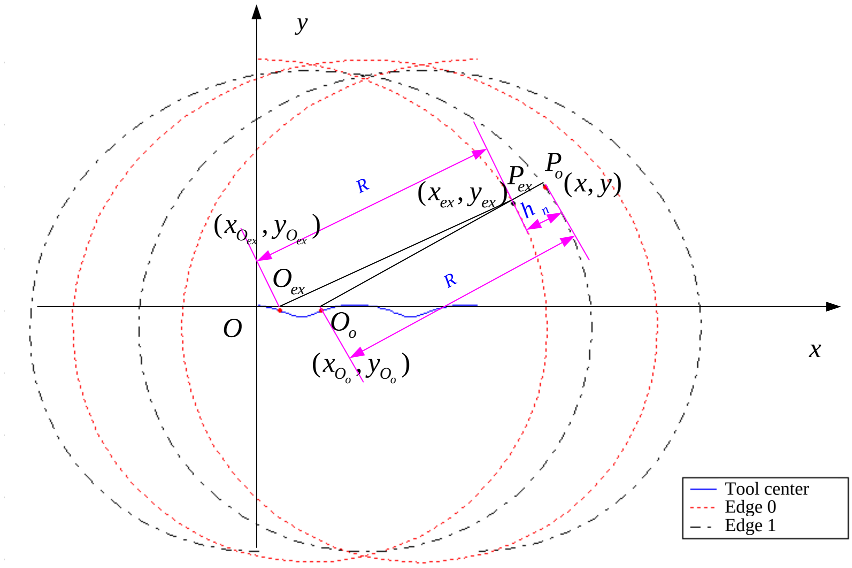

Figure 3. Schematic Diagram of Cutting Edge Trajectories

Instantaneous uncut chip thicknesses in the direction of the X-axis h_n could be calculated by the positions of the two cutting edges (starting time t = 0), as shown in equation (15) (edge k in front) and equation (16) (edge k+1 in front). This is the same as the definition of feed per tooth in conventional milling.

$$\begin{aligned} h_n &= x(\pi/2\omega + 2\pi/\omega K, k+1) - x(\pi/2\omega, k) \\ &= f_x(\pi/2\omega + 2\pi/\omega K) + R\sin[\omega(\pi/2\omega + 2\pi/\omega K) - 2\pi(k+1)/K] \\ &+ r\sin[\omega(\pi/2\omega + 2\pi/\omega K) + \gamma_0] - f_x(\pi/2\omega) - R\sin[\omega(\pi/2\omega) - 2\pi k/K] \\ &- r\sin[\omega(\pi/2\omega) + \gamma_0] \end{aligned} \tag{15}$$

$$\begin{aligned} h_n &= x(\pi/2\omega + 4\pi/\omega K, k) - x(\pi/2\omega + 2\pi/\omega K, k+1) \\ &= f_x(\pi/2\omega + 4\pi/\omega K) + R\sin[\omega(\pi/2\omega + 4\pi/\omega K) - 2\pi k/K] \\ &+ r\sin[\omega(\pi/2\omega + 4\pi/\omega K) + \gamma_0] - f_x(\pi/2\omega + 2\pi/\omega K) \\ &- R\sin[\omega(\pi/2\omega + 2\pi/\omega K) - 2\pi(k+1)/K] - r\sin[\omega(\pi/2\omega + 2\pi/\omega K) + \gamma_0] \end{aligned}$$

Replace $2\pi f_x/\omega K$ by feed rate per tooth f_t, and express h_n with the sign ξ. Equation (15) and (16) can be reduced to:

$$\xi = f_t - \left|2r\cos\gamma_0\right| \tag{17}$$

Equation (17) can be used as the criterion of single edge cutting phenomenon. When feed rate per tooth f_t, tool eccentricity length r, and tool eccentricity angle γ_0 satisfy $f_t<|2r\cos\gamma_0|$, the criterion value $\xi<0$, only one edge can remove material effectively, which is so-called single edge cutting phenomenon. Single edge cutting phenomenon also may appear in conventional milling. However, due to the large feed per tooth, single edge cutting phenomenon almost never appeared. The probability of single edge cutting phenomenon is very high in micro-milling. Single edge cutting cause one edge wear faster than the other one, as shown in Figure4. From Figure 4 it can be seen clearly that since single edge cutting phenomenon, only one edge wear, and the other one is almost no wear.

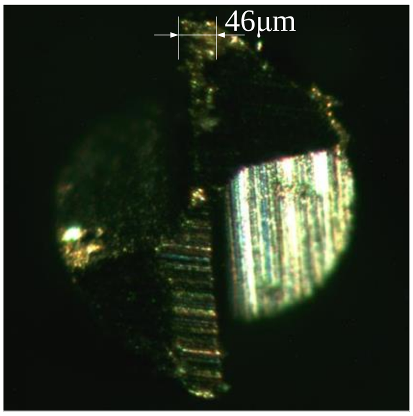

Figure 4. Tool Wears in Micro-milling

3. Tool Eccentricity Parameters Identification Method

Tool eccentricity initial position is shown in Figure 5a). Edge 0 rotates around the spindle axis is shown in red dashed line, and Edge 1 rotates around the spindle axis is shown in blue dotted line. The rotation radius of the edges can be calculated by the following equations:

$$\begin{aligned} R_0 &= [(R + r\sin\theta)^2 + r^2\sin^2\theta]^{1/2} \\ R_1 &= [(R - r\sin\theta)^2 + r^2\sin^2\theta]^{1/2} \end{aligned} \tag{18}$$

So, the edge circles can be expressed by the following equations:

$$\begin{aligned} X_0{}^2 + Y_0{}^2 &= R^2 + 2Rr\sin\theta + r^2 \\ X_1{}^2 + Y_1^2 &= R^2 - 2Rr\sin\theta + r^2 \end{aligned} \tag{19}$$

where, X_0, Y_0 are the coordinates of edge 0; X_1, Y_1 are the coordinates of edge 1; R is tool radius; r is tool eccentricity length; θ is tool eccentricity angle. The analytic expression of line A_0B_1 is

$$X = r\cos\theta \tag{20}$$

Simultaneous equation (19) and (20), the coordinates of point A_0 ($r\cos\theta$, $R+r\sin\theta$), A_1 ($r\cos\theta$, $-R+r\sin\theta$) and B_1 ($r\cos\theta$, $R-r\sin\theta$) can be calculated. So, the length of line segment A_0B_1 is:

$$l_1 = 2r\sin\theta \tag{21}$$

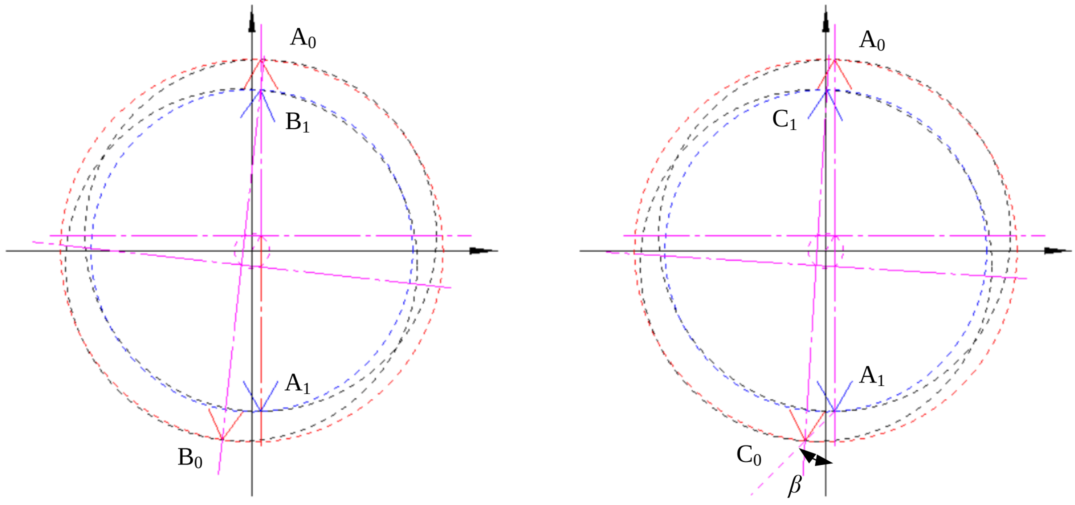

a) b)

Figure 5. Edges Trajectories

Edge 0 is rotated to point C_0 (X_{C0}, Y_{C0}), then the angle of line A_1C_0 and Y-axis is β. Establish the analytic expression of line A_1C_0, and substitute A_1's coordinates into the expression, and then the following equation is obtained as:

$$Y = X\tan\beta - R + r(\sin\theta - \tan\beta\cos\theta) \tag{22}$$

Simultaneous equation (21) and (22), the coordinates of point C_0 are expressed by the following equations:

$$\begin{aligned} X_{C0} &= \frac{m\tan\beta - [n(1+\tan^2\beta) - m^2]^{1/2}}{1+\tan^2\beta} \\ Y_{C0} &= -\frac{[n(1+\tan^2\beta) - m^2]^{1/2}\cdot\tan\beta + m}{1+\tan^2\beta} \end{aligned} \tag{23}$$

where,

$$\begin{aligned} m &= R - r(\sin\theta - \tan\beta\cos\theta) \\ n &= R^2 + 2Rr\sin\theta + r^2 \end{aligned} \tag{24}$$

Substitute $a=r\cos\theta$ and $b=-R+r\sin\theta$ into equation (24), then $m=a\tan\beta-b$, $n=4R^2+4Rb+a^2+b^2$, and

$$\begin{aligned} X_{C0} &= \frac{(a\tan\beta - b)\tan\beta - [4R(R+b)(1+\tan^2\beta) + (a+b\tan\beta)^2]^{1/2}}{1+\tan^2\beta} \\ Y_{C0} &= -\frac{[4R(R+b)(1+\tan^2\beta) + (a+b\tan\beta)^2]^{1/2}\cdot\tan\beta + a\tan\beta - b}{1+\tan^2\beta} \end{aligned} \tag{25}$$

So, the length of line segment A_1C_0 is:

$$
\begin{aligned}
l_2 &= [(X_{A1}-X_{C0})^2+(Y_{A1}-Y_{C0})^2]^{1/2} \\
&= \left\langle \left. \begin{array}{l} \{[4R(R+b)(1+\tan^2\beta)+(a+b\tan\beta)^2]^{1/2}\cdot(2a-2b\tan\beta) \\ +(1+\tan^2\beta)(4R^2+4Rb+2b^2)+(2a^2+2b^2)\} \end{array} \right/ (1+\tan^2\beta) \right\rangle^{1/2} \qquad (26)
\end{aligned}
$$

Similarly, multiple distance equations (l_3, l_4, … l_n) which are expressed by tool eccentricity parameters could be obtained. Calculate the standard deviation square sum of theoretical distances and measured distances by iterative algorithm (tool eccentricity length iterative range is from 0 to 10 micron; tool eccentricity angle iterative range is from 0 to 360 degree). When the standard deviation square sum is the minimum one, that tool eccentricity parameters are the actual parameters. The flow of iterative algorithm is shown in Figure 6.

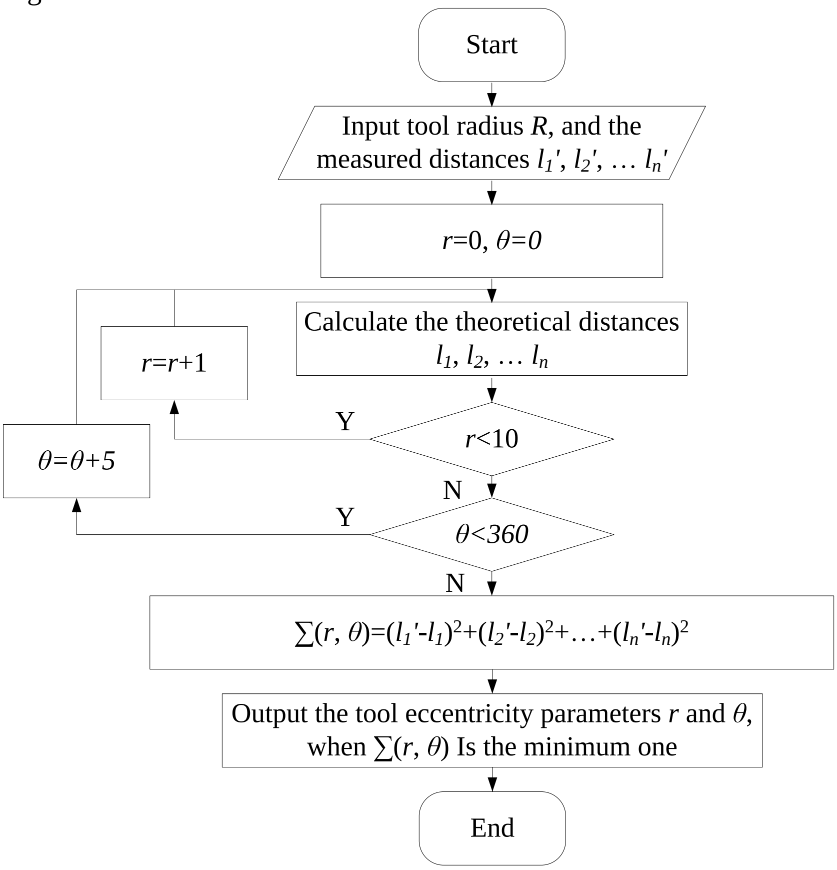

Figure 6. Iterative Algorithm for Tool Eccentricity Parameters Identification

4. Measuring Experiment

4.1 Model Parameters Measuring

Set the displacement sensor along the Y-axis, as shown in Figure 7. Slowly counterclockwise rotate the tool, and get the minimum value of displacement sensor. Then slowly counterclockwise rotates about 180°, and get the minimum value of displacement sensor again. The distance of the edges l_1' could be calculated by the difference of the two values. The distance l_2' could be calculated by setting the displacement sensor and Y-axis of angle β, and repeats above steps. Other distances (l_3', l_4', … l_n') could be obtained by the similarly method.

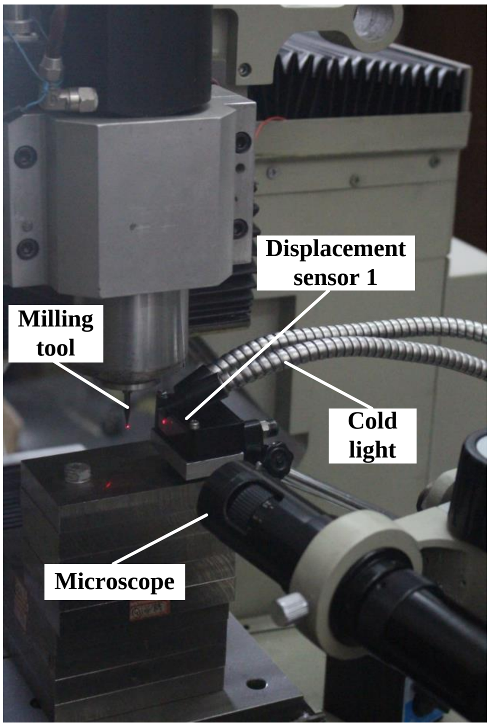

Figure 7. Measuring Experiment

4.2 Recognized Results Verifying

A self-developed 5-axis micro-milling machine tool [11], Pingdin™ two edges micro-milling tool and aluminum alloy AlCu4Mg1 are used to verify the recognized results. The milled hole diameter is 512μm, which is measured by Olympus™ laser scanning confocal microscope OLS3000, as shown in Figure 8. The tool diameter is 504μm, which is also measured by OLS3000. Tool eccentricity length and angle are 6μm and 50°, which are recognized by the proposed method. The diameter larger edge circle is 513.2μm, which is calculated by equation (18). It can be seen that the measured and calculated hole diameters are quite matched, and this result could verify the proposed primarily.

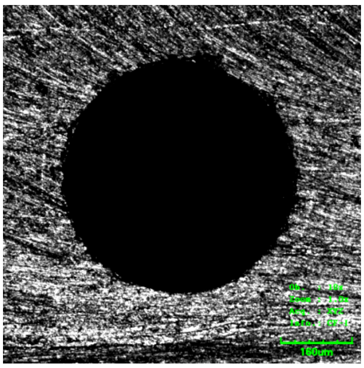

Figure 8. Confocal Microscopy Images of Milled Hole

5. Conclusions

In this paper, the influence of tool eccentricity is analyzed, and a tool eccentricity parameters identification method is proposed in micro-milling. Firstly, the tool eccentricity is defined, and cutting edge trajectory model is established. Secondly, the effect of tool eccentricity is analyzed, and a criterion of single edge cutting phenomenon is proposed. Finally, a tool eccentricity parameters identification method is proposed which is based on analytic geometry. In this method, tool eccentricity parameters are calculated by iterative algorithm. The measurement of milled hole diameter which is observed by confocal microscopy confirmed the validity and the applicability of the identification method.

Acknowledgements

This project is supported by National Natural Science Foundation of China (Grant No. 51605118) and "the Fundamental Research Funds for the Central Universities" (Grant No. HIT. NSRIF. 201642).

References

[1] K. P. Zhu, Y. S. Wong and G. S. Hong, J. Mechanical Systems and Signal Processing. 23, 547 **(2009)**
[2] Z. Y. Han, X. Zhang, Y. Z. Sun and H. Y. Fu, J. Advanced Science Letters. 4, 1387 **(2011)**
[3] M. L. Zheng and Y. H. Fan, J. Journal of Harbin University of Science and Technology. 16, 22 **(2011)**
[4] H. S. Feng and C. H. Menq, J. International Journal of Machine Tools and Manufacture. 34, 697 **(1994)**
[5] C. C. Tai and K. H. Fuh, J. International Journal of Machine Tools and Manufacture. 34, 959 **(1994)**
[6] W. Nakkiew, C. W. Lin and J. F. Tu, J. International Journal of Machine Tools and Manufacture. 46, 877 **(2006)**
[7] K. A. Hekman and S. Y. Liang, J. Mechatronics. 7, 1 **(1997)**
[8] M. Wan, W. H. Zhang, J. W. Dang and Y. Yang, J. International Journal of Machine Tools and Manufacture. 49, 1144 **(2009)**
[9] J. H. Ko, W. S. Yun, D. W. Cho and K. F. Ehmann, J. International Journal of Machine Tools and Manufacture. 42, 1595 **(2002)**
[10] X. Zhang, Z. Y. Han, H. Y. Fu and Y. Z. Sun, J. Advanced Science Letters. 4, 1776 **(2011)**
[11] X. Zhang, Z. Y. Han, Y. Z. Sun and H. Y. Fu, J. Key Engineering Materials. 431-432, 78 **(2010)**

